Engineering Structures 32 (2010) 2950–2958

Contents lists available at ScienceDirect

Engineering Structures

journal homepage: www.elsevier.com/locate/engstruct

Performance-based plastic design method for buckling-restrained braced frames

Dipti R. Sahoo [a], Shih-Ho Chao [b,*]

[a] Department of Civil Engineering, Indian Institute of Technology Bhubaneswar, Orissa 750013, India

[b] Department of Civil Engineering, University of Texas at Arlington, TX-76019, USA

ARTICLE INFO

Article history:
Received 21 March 2010
Received in revised form
25 May 2010
Accepted 25 May 2010
Available online 17 July 2010

Keywords:
Buckling-restrained braced frames
Performance-based design
Seismic
Yield mechanism
Energy–work balance
PBPD

ABSTRACT

This paper presents a performance-based plastic design (PBPD) methodology for the design of buckling-restrained braced frames (BRBFs). The design base shear is obtained based on energy–work balance using pre-selected target drift and yield mechanism. Three low-to-medium rise BRBFs (3-story, 6-story and 9-story) were designed by the proposed methodology and their seismic performance was evaluated through extensive nonlinear time-history analyses using forty ground motions representing the DBE and the MCE hazard levels. Both isotropic and kinematic hardening characteristics of buckling-restrained braces were considered in the modeling of their force–deformation behaviors. All BRBFs considered in this study reached the intended performance objectives in terms of yield mechanisms and target drift levels. Since PBPD is a direct design method, no iterations were carried out to achieve the performance objectives of BRBFs.

1. Introduction

Buckling-restrained braced frames (BRBFs) are emerging systems used as primary lateral load resisting systems for buildings in high seismic areas. The main characteristics of buckling-restrained braces (BRBs) are enhanced energy dissipation potential, excellent ductility, and nearly symmetrical hysteretic response in tension and compression. Different types of BRBs have been developed and tested in United States and elsewhere in recent years [1]. A typical BRB consists of a yielding steel core encased in a mortar-filled steel hollow section to restrain buckling, non-yielding and buckling-restrained transition segments, and non-yielding and unrestrained end zones (Fig. 1). The length of the buckling-restrained (core) segment of BRB is about 60%–70% of the total length between work points (e.g [2,3]). Axial forces in BRBs are primarily resisted by steel cores which are laterally braced continuously by the surrounding mortar and steel encasement to avoid their buckling under compressive loads. This allows the steel core to yield in tension and compression, thereby significantly increasing the energy dissipation capacities of BRBs as compared to conventional steel braces. A more comprehensive background on BRBs can be found elsewhere [4]. Recent analytical and experimental studies [5,6] have shown that BRBFs can be used to overcome several potential problems associated with the conventional steel concentrically braced frames (CBFs), such as, sudden degradation in strength and stiffness, reduced energy dissipation capacity, and limited ductility. Because of the nearly symmetrical behavior of BRBs in tension and compression resulting in much smaller unbalanced vertical brace forces, BRBFs also require smaller beam sections as compared to conventional CBFs with chevron bracing configurations [7].

It is expected that BRBFs will experience large inelastic deformation when subjected to major earthquake ground motions. However, most current seismic design methods are still based on the elastic analysis approach and use indirect ways to account for inelastic behavior. As such, the current performance-based design methodology relies heavily on an iterative "Assess Performance", "Revision Design, and "Assess Performance" process to reach a design capable of achieving the intended performance [8]. On the other hand, the proposed design methodology addresses the need for developing a systematic design approach that results in predictable and targeted seismic performance of structures under stated levels of seismic hazards. This in turn minimizes, if not totally eliminates, the assessment and redesign tasks as required by current code provisions.

2. Objectives and scope

Since Housner [9] applied the concept of energy into seismic design of structures, much effort has been made in the field of energy-based seismic engineering. A recently developed performance-based plastic design (PBPD) methodology is considered in the present study in which inelastic characteristics of structural components are directly considered in the design to achieve

* Corresponding author. Tel.: +1 817 272 2550; fax: +1 817 272 2630.
E-mail address: shchao@uta.edu (S.-H. Chao).

0141-0296/$ – see front matter © 2010 Elsevier Ltd. All rights reserved.
doi:10.1016/j.engstruct.2010.05.014

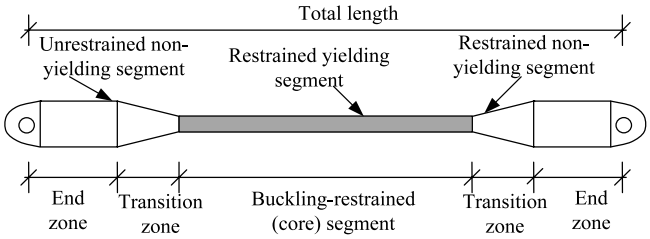

Fig. 1. Components of a typical BRB.

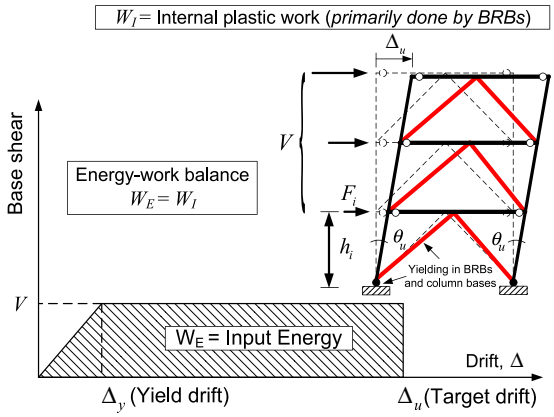

Fig. 2. Energy–work balance concept.

the desired performance objectives of BRBFs. This design methodology has already been successfully applied to various steel structural framing systems [10–12]. This study presents an application of PBPD method to low-to-medium rise BRBFs with both chevron and X-shaped bracing configurations. The robustness of proposed design methodology is verified through a series of nonlinear time-history analysis using PERFORM-3D [13] for both design basis earthquake (DBE, 10% probability of exceedance in 50 years, return period = 475 years) and maximum considered earthquake (MCE, 2% probability of exceedance in 50 years, return period = 2475 years) hazard level ground motions.

3. Performance-based plastic design (PBPD)

3.1. Design philosophy

The detailed underlying methodology of PBPD can be found elsewhere [14]. In summary, PBPD concept uses pre-selected target drift and yield mechanism as design criteria. In this method, the design base shear is computed using an energy–work balance concept where the energy needed to push an equivalent elastic–plastic single-degree-of-freedom system up to the target drift level is calculated as a fraction of elastic input energy obtained from the selected elastic design spectra (Fig. 2). The design base shear for a structure can be expressed by [14]:

$$V/W = \left(-\alpha + \sqrt{\alpha^2 + 4\,(\gamma/\eta)\,S_a^2}\right)/2 \tag{1}$$

where, V is the design base shear; W is the total seismic weight of the structure; S_a is the spectral response acceleration obtained from code design spectrum; α is a dimensionless parameter depends on fundamental period (T), modal properties, and pre-selected plastic drift ratio (θ_p) and can be given by:

$$\alpha = \left(\sum_{i=1}^{n}(\beta_i - \beta_{i+1})h_i\right)\left(\frac{w_n h_n}{\sum_{j=1}^{n} w_j h_j}\right)^{0.75T^{-0.2}}\left(\frac{8\theta_p\pi^2}{gT^2}\right). \tag{2}$$

In the above equation, β_i represents the shear distribution factor at ith level and can be expressed as $\beta_i = (\sum_{j=i}^{n} w_j h_j / w_n h_n)^{0.75T^{-0.2}}$; β_{i+1} represents the shear distribution factor at $(i+1)$th level; w_j is the seismic weight at jth level; h_i is the height at ith level from the base; h_j is the height at jth level from the base; h_n is the height of roof level from the base; w_n is the seismic weight at roof level. The energy modification factor (γ) given in Eq. (1) can be related to structural ductility factor ($\mu_s = \Delta_u/\Delta_y$) and ductility reduction factor, R_μ, by the following expression [14]:

$$\gamma = (2\mu_s - 1)/R_\mu^2. \tag{3}$$

The value of R_μ for a structural system can be determined by using the $R_\mu - \mu_s - T$ relationship, such as an inelastic spectrum proposed by Newmark and Hall [15], as shown in Fig. 3(a). Several structural systems exhibit significant reduction in strength and stiffness resulting unstable and "pinched" hysteresis response at the higher inelastic deformation levels. This reduction in energy dissipation capacity can also be accounted in the design by using an energy reduction factor ($\eta = A_1/A_2$) as shown in Fig. 3(b). Since BRBFs exhibit full and stable hysteretic response, the value of η can be assumed as unity in Eq. (1).

3.2. Step-by-step design procedure

A step-by-step PBPD procedure of a typical BRBF system is summarized as follows:

1. Select intended target drift ratio, θ_u, and desired yield mechanism for expected hazard level. Estimate fundamental period (T) for the system from the mass and stiffness properties. Empirical formulae based on codes (e.g. ASCE 7-05 [16]) can also be used to estimate the expected fundamental period of the system.
2. Compute the plastic drift ratio (θ_p) by deducting the yield drift ratio (θ_y) from the pre-selected target drift ratio (θ_u). The upper-bound values of yield drift ratio for BRBFs can be obtained by conventional pushover analysis based on code-based lateral force distributions. Based on extensive nonlinear dynamic analyses, Sahoo and Chao [17] proposed a simple expression for yield drift ratio as a function of total height (H) of BRBFs and can be expressed as follows:

$$\theta_y(\%) = 0.2 + H/155 \quad (\text{Unit of } H \text{ is meter}). \tag{4}$$

3. Compute the value of α from the modal properties and the plastic drift level using Eq. (2) and estimate the value of γ using Eq. (3). Determine the design base shear ratio (V/W) of structure using Eq. (1) and distribute the lateral load at various story levels based on a lateral load distribution proposed by Chao et al. [18] that accounts the inelastic behavior. The magnitude of lateral load at ith story level was obtained as the design base shear times $(\beta_i - \beta_{i+1})$, where β_i is defined earlier and $\beta_{i+1} = 0$ at the roof level.
4. Determine brace sizes by resolving the computed story shear in the direction of braces for the nominal values of yield strengths of BRBs. The compressive yield strength of BRBs can be conservatively assumed as 10%–25% higher than their tensile yield strengths [19].
5. Determine the section sizes for beams and columns (termed as non-yielding members) of BRBFs based on capacity design philosophy for the maximum demand expected from the BRBs at the ultimate states. Check the compactness and lateral bracing requirements of these members as per the AISC Seismic Provisions [20].

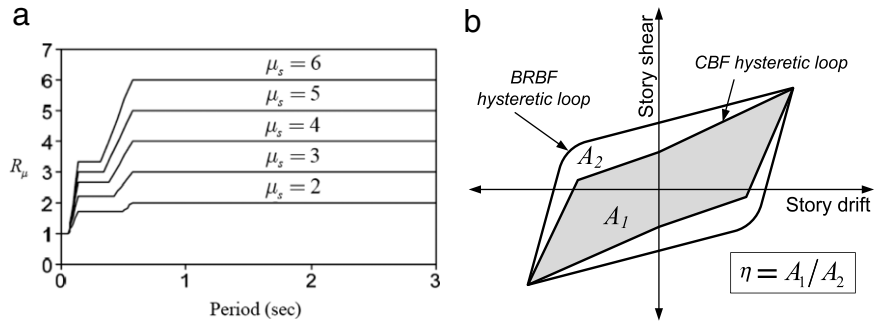

Fig. 3. (a) Relationship between R_μ, μ_s, and T [15]. (b) Definition of energy reduction factor, η.

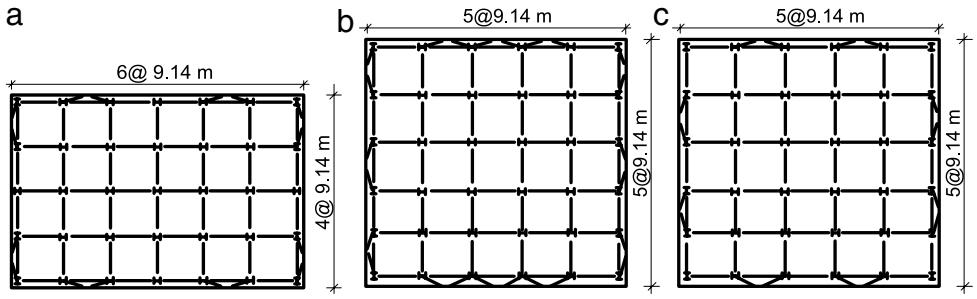

Fig. 4. Plan views of study buildings (a) 3-story (b) 6-story (c) 9-story.

4. Building models

Three buildings (i.e., 3-, 6-, and 9-story) were considered for design and evaluation of their seismic performance in this study. All buildings were located on firm soil (site classification *D*) in Los Angeles. The dimensions and floor masses for both 3- and 6-story buildings were exactly matched with those adopted by Sabelli [5] for braced frame studies. However, plan layout and floor masses for the 9-story building were adopted from Gupta and Krawinkler [21]. As shown in Fig. 4, typical bay width in each direction of all buildings was 9.14 m (30 ft). The 6-story building had a total of six bays with BRBs in each direction, whereas both 3- and 9-story buildings had four bays with BRBs in each direction. All braced bays were located at the perimeter of buildings. Except for the first story height of 5.49 m for the 6- and 9-story buildings, typical story height for all buildings was 3.96 m (Fig. 5). Seismic weights for the 3-, 6-, and 9-story buildings were 28 910 kN, 59 295 kN, and 97 325 kN, respectively. The spectral acceleration values at 0.2 s (S_{DS}) and 1 s (S_{D1}) were 1.39 and 0.77*g* for both the 3- and 6-story BRBFs [5], whereas the corresponding values used for the 9-story BRBF were 1.11 and 0.61 g [21].

4.1. Design base shear for BRBFs

Table 1 summarizes various parameters used to compute the design base shear for all BRBFs used in the present study. A target drift level of 1.75% was selected for all BRBFs leading to structural ductility factor, μ_s, ranging from 3.94 to 6.25. The computed range of ductility was smaller than the brace ductility capacities according to prior experimental studies [6,19]. A pinned beam–column-brace connection, as illustrated in Fig. 5, was used at all story levels of both 3- and 6-story BRBFs to avoid undesirable connection failures due to induced moments resulted from unbalanced brace forces [6]. However, for the 9-story BRBF with X-configuration BRBs, pinned beam-to-column connections were used at the story levels where unbalanced brace forces were present, otherwise rigid connections where unbalanced brace forces were absent.

Response modification factor, *R*, equal to 8 was used in the original code-compliant design of the 3- and 6-story BRBFs, whereas *R* equal to 7 was used in the original code-compliant design of the 9-story BRBF [20]. However, the change in value of *R* from 6 to 8 in the design does not change the overall seismic performance of BRBFs significantly [5]. For all cases, the occupancy importance factor, *I*, was assumed as unity for all code-compliant design. Note that, *R* and *I* factors are not explicitly required in the PBPD methodology. As expected, the design force level increases with the increase in the value of *I* in an attempt to lower down the drift and ductility demands of structures for a given level of ground shaking [22,23]. However, such procedure cannot be considered as a direct design method to achieve the intended purpose, such as damage control. The reduction of potential damage in structures should better be handled by using appropriate drift limitations directly. In that regard, the approach for calculating the design base shear in the PBPD method uses target drift as the governing parameter, which should account for occupancy importance. The values of base shear coefficient, C_s, were 0.174 for the 3- and 6-story BRBFs and 0.085 for the 9-story BRBF, if designed based on current code provisions [16]. However, the design base shear coefficients as per the PBPD methodology were 0.158, 0.100 and 0.054 for the 3-, 6- and 9-story BRBFs, respectively. Thus, the PBPD methodology uses smaller design base shear as compared to current codes with the maximum reduction in design base shear as 43% and 36% for the 6-story and 9-story BRBFs, respectively. Since the collapse prevention rather than drift control is the governing performance criteria for structures under MCE hazard level, the performance of BRBFs designed for DBE level was also investigated under MCE ground motions in this study.

4.2. Design of frame members

The desired yield mechanism of BRBFs requires that yielding should be limited to braces and plastic hinges at the bases of first story columns only (Fig. 2). All frame members were designed based on their nominal material strengths. The maximum axial force demand on BRBs at the target drift level was obtained from

Table 1
Design parameters used in the computation of design base shear for PBPD BRBFs.

No.	Parameters	3-story	6-story	9-story	Note
1	Target drift ratio, θ_u (%)	1.75	1.75	1.75	Pre-selected
2	Total frame height (m)	11.9	25.3	37.2	Fig. 5
3	Yield drift ratio, θ_y (%)	0.28	0.37	0.44	Eq. (4)
4	Fundamental period (s)	0.43[a]	0.77[a]	1.03[a]	Ref.: ASCE 7-05 [16], $C_u = 1.4$
5	Inelastic drift ratio, θ_p (%)	1.47	1.38	1.31	(5) = (1)−(3)
6	Ductility reduction factor, R_μ	4.79	4.78	3.94	Fig. 3(a)
7	Structural ductility factor, μ_s	6.25	4.78	3.94	(7) = (1)/(3)
8	Energy modification factor, γ	0.51	0.38	0.44	Eq. (3)
9	Spectral acceleration, S_a	1.39	1.00	0.59	
10	Base shear coefficient, V/W	0.158	0.100	0.054	V = 1170 kN (3-story); 1005 kN (6-story); 1350 kN (9-story)

[a] Based on computer analysis, fundamental periods are 0.65 s. (3-story), 1.03 s (6-story), and 1.44 s (9-story).

Table 2
Details of BRBs and structural sections used in PBPD BRBFs.

Members	Story	3-story	6-story	9-story
BRBs (Tensile yield strengths, kN)	1st	1093	1093	1137
	2nd	937	885	942
	3rd	624	833	907
	4th	–	729	856
	5th	–	572	789
	6th	–	364	703
	7th	–	–	596
	8th	–	–	464
	9th	–	–	296
Column sections	1st–2nd	W14 × 90	W14 × 145	W14 × 233
	3rd–4th	W14 × 90	W14 × 145–W14 × 74	W14 × 145
	5th–6th	–	W14 × 74	W14 × 90
	7th–9th	–	–	W14 × 61
Beam sections	–	W14 × 34 (All floors)	W14 × 30 (1st–3rd) W14 × 26 (4th–6th)	W16 × 40 (All floors)

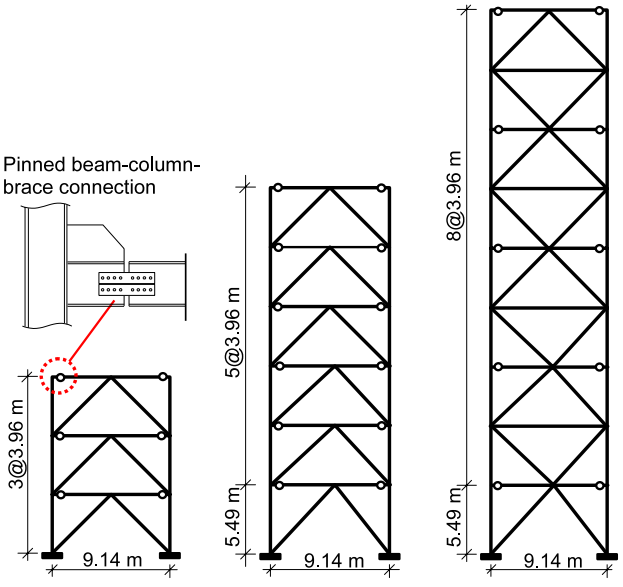

Fig. 5. BRBFs and their brace-beam–column connections (a) 3-story (b) 6-story (c) 9-story.

the expected story shear by using a lateral force distribution proposed by Chao et al. [18]. Fig. 6 shows a step-by-step procedure for design of frame members of BRBFs with chevron bracing configuration. Similar procedure with minor modifications in brace unbalanced forces can be followed for design of BRBFs with braces in X-configuration. Brace sizes were determined by assuming nominal yield strength of braces as 36 ksi and strength reduction factor of 0.9 for both tension and compression [24]. However, the maximum force demands on beams and columns was computed based on expected yield and ultimate strengths of BRBs in tension and compression by applying material overstrength factor (R_y), compression adjustment factor (β) and tension adjustment factor (ω) to the nominal yield strength values. Since these values depend on the type of braces used in BRBFs, two different sets of values were considered in this study. For 3- and 6-story BRBFs, the values of R_y, β, and ω were considered as 1.3, 1.1, and 1.4, respectively. The corresponding values of R_y, β, and ω for 9-story BRBF were 1.1, 1.22, and 1.45, respectively [25]. For all cases, nominal yield strength of materials used in beams and columns was 50 ksi with the value of R_y as 1.1. Due to the introduction of pinned beam-to-column connection (i.e., beam splice), all columns of BRBFs were designed for axial loads only. It was later shown in nonlinear time-history analyses that additional moments induced by column bending have negligible effect on the overall seismic behavior. Table 2 summarizes the details of BRBs and beams and columns at various story levels of BRBFs. Chao et al. [18] showed that relative story shear distribution for a braced frame using a lateral load distribution factor of 0.75 represents an upper bound to nonlinear dynamic analysis results and leads to more uniform deformations of elements as well as stories over the height of the structure as compared to a factor of 0.50. Hence, all members of BRBFs in this study are designed for a load distribution factor of 0.75.

5. Seismic performance of BRBFs

5.1. Modeling and analysis

The seismic performance of BRBFs was evaluated by nonlinear analysis using a computer program PERFORM-3D [13]. Beams and columns were modeled as standard frame elements with plastic hinges lumped at both ends. Both axial-moment (P-M-M) and moment–rotation hinges were assigned to all beam and column

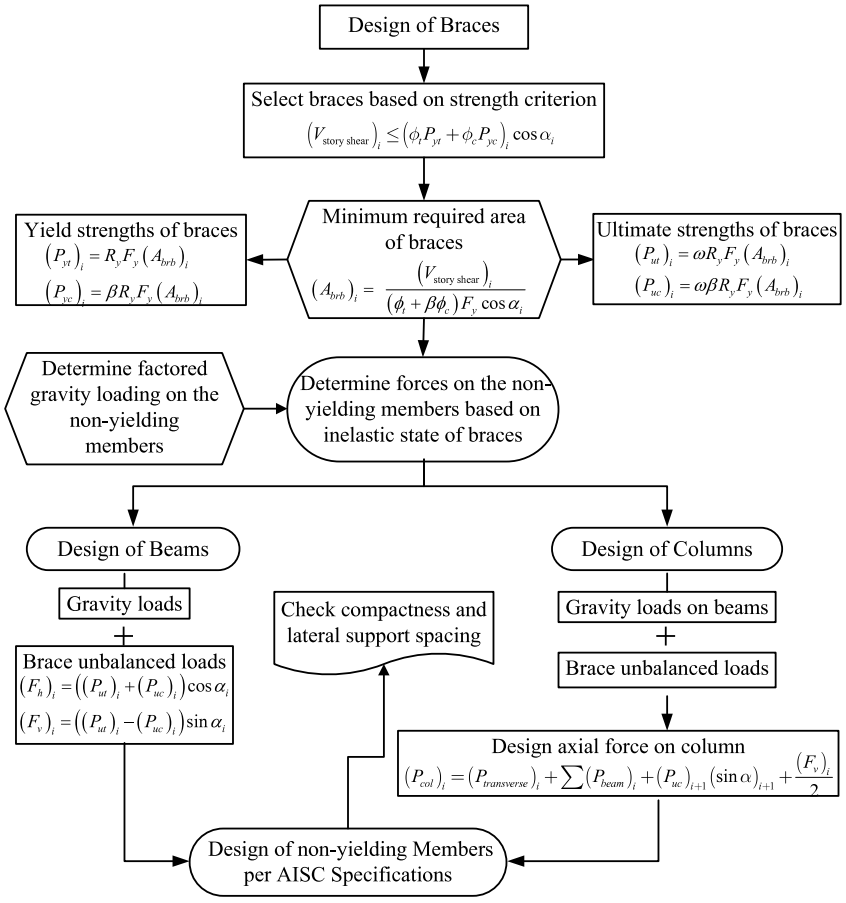

Fig. 6. Flowchart for design of BRBFs with chevron bracings (Note: $\phi_t = \phi_c$ as per AISC Specifications [24]; α = Angle of inclination of brace with horizontal; P_{yt} and P_{yc} are BRB yield strengths in tension and compression; P_{ut} and P_{uc} are BRB ultimate strengths in tension and compression; F_h and F_v are horizontal and vertical loads on beams; $P_{\text{transverse}}$ = Axial load on column from transverse direction; P_{beam} = Axial load on column from beam gravity loading; $V_{\text{storyshear}}$ = Design story shear; A_{brb} = Cross-sectional area of BRB).

elements assuming that they would carry significant axial force with biaxial bending. However, since all analyses were carried out on two dimension frame models, there would be no biaxial bending of frame members. For the 9-story BRBFs, beam-to-column connections were assumed as rigid where BRBs and gusset plates were present; otherwise these connections were assumed as pined. For both 3- and 6-story BRBFs, moment releases were used at beam ends to simulate the presence of beam splice (Fig. 5). Addition of the beam splice can eliminate the moment-frame action and prevent failure in the gusset regions [3,26]. All columns were assumed to be perfectly fixed to the ground.

P-Delta effect due to gravity loads resulted from gravity frames was modeled by an equivalent continuous column representing all gravity columns associated with the frame. The magnitude of axial load in these equivalent columns was computed from the total building weight (exclusive of tributary gravity load to the braced frames) and the number of braced frames along a particular direction. Lateral stiffness and strength of these columns at each story level represent the sum of respective values of all gravity columns at that story level assuming their weak axis bending. These columns were pinned at their bases and constrained to match the frame displacement at each floor level by using pin-ended rigid beams. For time-history analyses, Rayleigh damping of 2% was used in all modes of structures.

Standard BRB elements were chosen to model all braces of BRBFs in PERFORM-3D [13]. In general, the area of transition (elastic) and end zones of BRBs are larger than that of the core (restrained yielding) segment to limit the yielding to the core segment only. As shown in Fig. 7(a), the area of transition and end segments of BRBs were assumed as 160% and 220% of the area of the core segment, respectively. Similarly, the length of transition and end segments were assumed as 6% and 24% of the total length of BRB [2]. Considering the variation of cross-sectional area along the length of brace, the effective axial stiffness of BRB (K_{eff}) should consider stiffness of all segments and can be expressed as follows [2].

$$(K_{\text{eff}}) = EA_cA_jA_t/(A_cA_jL_t + L_cA_jA_t + A_cL_jA_t). \quad (5)$$

Elastic modulus of steel was considered as 200 GPa to compute the axial stiffness of BRBs. The post-yield stiffness of BRBs in tension can be different from that in compression depending on the type of outer casing and confining material used for lateral support to brace core [19,27]. In this study, the post-yield stiffness of core segments in tension and compression was assumed as 3% of their initial stiffness. It should be noted that, in practice, the presence of gusset plates may alter the lateral stiffness of BRBFs to some extent [3]. Both isotropic and kinematic hardening characteristics were considered in the modeling of force–deformation response of BRBs. Various hardening parameters were obtained by comparing the hysteretic response of a typical BRB from PERFORM-3D [13] with the component test results [19] as shown in Fig. 7(b). To monitor the magnitude of plastic displacements of BRBs under various ground motions, the values of maximum ductility of BRBs were assumed as 15 and 25 for DBE and MCE level analyses, respectively. Similarly, the respective values of cumulative plastic displacement of BRBs were fixed as 200 and 400 times their yield displacements. These ductility values are quite conservative since component test results showed that BRBs can have maximum

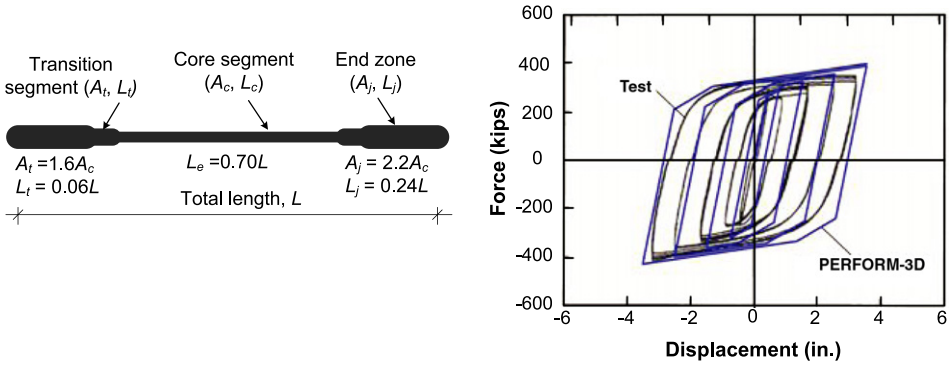

Fig. 7. (a) Modeling of different segments of BRBs (b) Calibration of force–deformation characteristics of BRBs in PERFORM-3D (1 kips = 4.448 kN; 1 in. = 25.4 mm).

ductility and cumulative ductility capacities of 26 [6] and 1700 [19], respectively, without any degradation in their strength and stiffness.

As stated earlier, the seismic response of BRBFs was evaluated under two earthquake hazard levels, namely, design basis earthquake (DBE) and maximum considered earthquake (MCE). Two suites of ground motions records developed by Somerville et al. [28] for a hypothetical site in downtown Los Angeles with a probability of exceedance of 10% and 2% in 50 years were selected for nonlinear time-history analysis. These acceleration time histories were derived from historical recordings or from physical simulations and were modified such that their mean response spectrum matches the 1997 NEHRP design spectrum. A total of forty records were obtained from twenty ground motions in both fault-parallel and fault-normal orientations. The magnitude of earthquakes varied from 6 to 7.4 with the hypocentral distance of earthquakes varied from 1.2 to 36 km.

5.2. Analysis results and discussion

Nonlinear time-history analyses were carried out to evaluate the seismic performance of BRBFs, in terms of interstory drift ratio, residual drift ratio, yield mechanism and displacement ductility. Interstory (or residual) drift ratio was defined as the ratio of the interstory (or residual) displacement to the corresponding story height. Due to well-controlled drifts realized by the PBPD approach, no additional design force was used in the design to account for the *P*-Delta effect. A statistical analysis was carried out to evaluate the mean and standard deviation of drift ratios for all BRBFs. Fig. 8(a) shows the interstory drift response of all BRBFs under DBE level ground motions. The maximum value of interstory drift ratio for 3-story BRBF was 3.0% observed for LA13 ground motion. The mean and mean-plus-standard deviation values of interstory drift ratios for the 3-story BRBF varied from 1.44% to 1.62%, and 2.0% to 2.33%, respectively. Similarly, 6-story BRBF exhibited a maximum interstory drift ratio of 3.3% observed for LA09 ground motion. The mean and mean-plus-standard deviation values of interstory drift ratios for the 6-story BRBF varied from 1.15% to 1.73%, and 1.56% to 2.36%, respectively. The maximum interstory drift ratio for 9-story BRBF was 2.82% for LA03 ground motion, whereas the mean and mean-plus-standard deviation values of interstory drift ratios ranging from 1.03% to 1.72%, and 1.37% to 2.35%, respectively. The average values of maximum interstory drift ratio for 3-, 6- and 9-story BRBFs were 1.71%, 1.73% and 1.83%. Hence, all BRBFs reached the target drift level of 1.75% under DBE level ground motions even without any design iteration. Since drifts were well controlled by considering inelastic behavior directly in the design of these BRBFs, the *P*-Delta effect had no appreciable influence on their overall behavior. Unlike 3- and 6-story BRBFs, the distribution of interstory drift ratio was not fairly uniform over the building height for 9-story BRBF. The larger interstory drifts at the lower stories of 9-story BRBF indicated that BRBs at these story levels dissipated relatively larger seismic energy than those at upper stories.

Fig. 8(b) also shows the interstory drift response of BRBFs under MCE level ground motions. The maximum value of mean interstory drift ratio was about 3.5% for 3-story BRBF. Similarly, 6-story BRBF showed the maximum value of mean interstory drift ratio of 3.83% at the second story level which reduced to 2.08% at the sixth story level. The maximum value of mean interstory drift ratio of 9-story BRBF was 4.3% observed at the second story level and reduced to 1.31% at the roof level. Thus, BRBs in the lower stories of both 6- and 9-story BRBFs were subjected to larger drift demands under MCE level ground motions. However, since the collapse prevention rather than controlling maximum drift of BRBFs is the governing performance criteria for MCE level ground motions, the large values of interstory drift ratios did not hinder the applicability of BRBFs as primary seismic resisting systems since BRBFs with the beam–column-brace configuration shown in Fig. 5 have exhibited excellent seismic performance and sustain only minor yielding at story drift ratio up to 4.8% [6]. Hence, all BRBFs exhibited accepted overall performance of under MCE level ground motions even though they were designed for DBE level only.

Fig. 9(a) shows the residual drift ratio response of BRBFs under DBE level ground motions. The mean values of residual drift ratio for 3-story BRBF varied from 0.45% to 0.70%. The 6-story BRBF exhibited mean residual drifts ranging from 0.36% to 0.61%. For both 3- and 6-story BRBFs, the residual drift response was fairly uniform over the building height under DBE level ground motions. Similarly, the 9-story BRBF showed mean values of residual drift ranging from 0.27% to 0.67%. Similar to the interstory drift distribution, the residual drift distribution in 9-story BRBF was not uniform over the height. As shown in Fig. 9(b), both 3- and 6-story BRBFs under MCE level ground motions showed the mean values of residual drift ratio as about 1.7%. The maximum value for mean residual drift ratio was 2.28% for 9-story BRBF. It should be noted that the distribution of residual drift ratio in 9-story BRBF under the MCE level ground motions was different from that under DBE level ground motions and the BRBs at the lower stories dissipated significant amount of energy due to large deformations under MCE level earthquakes.

No plastic hinges were formed in beams and columns except the yielding at column bases in BRBFs under DBE level ground motions. Thus, the intended yield mechanism was achieved under the DBE hazard level. Under MCE level earthquakes, flexural yielding of beams and columns at different story levels of 9-story BRBFs was noticed because of larger strength and deformation demand. However, these members did not reach their ultimate deformation and load-carrying capacity which prevented these BRBFs from their complete collapse. Braces did not reach their maximum ductility and cumulative displacement ductility limits of 15 and

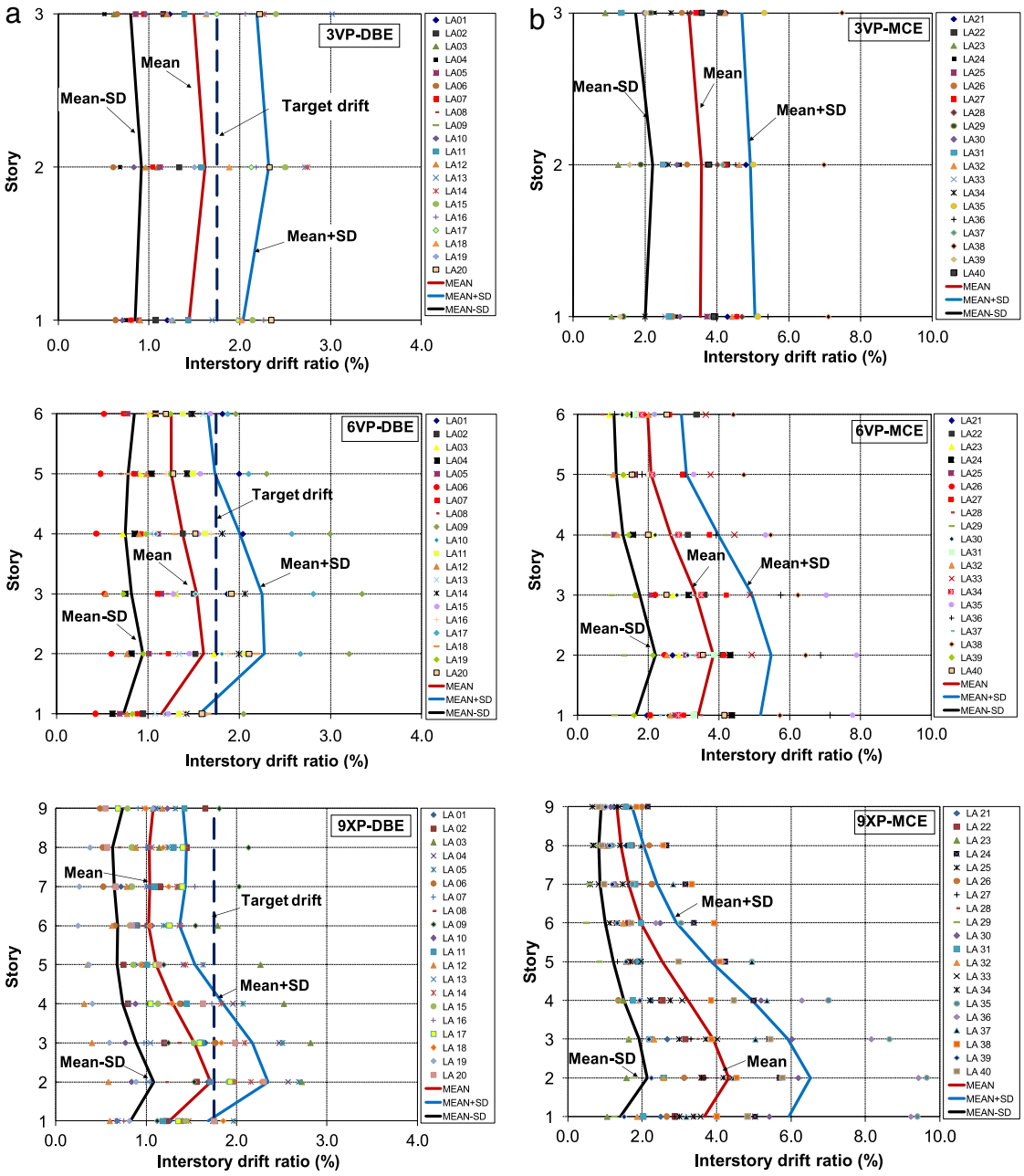

Fig. 8. Interstory drift response of BRBFs (a) DBE (b) MCE.

200, respectively, for all BRBFs under DBE level ground motions. The mean values of maximum ductility demand of BRBs were 7.3, 8.0, and 9.3 for 3-, 6-, and 9-story BRBFs, respectively. Similarly, the mean values of cumulative displacement ductility demand of BRBs under the DBE level ground motions were 24.5, 21.8, and 32.7 for 3-, 6-, and 9-story BRBFs, respectively. BRBs in all BRBFs also did not exceed their cumulative ductility demand of 400 under the MCE level ground motions. The mean values of maximum cumulative displacement ductility demands were 43.6, 48.7, and 47.2 for 3-, 6-, and 9-story BRBFs, respectively, under MCE level ground motions. Similarly, the mean values of maximum ductility demand of BRBs of 3-, 6-, and 9-story BRBFs under the MCE level ground motions were 17.2, 17.6, and 16.0, respectively, which indicates that mean values of maximum ductility demand of BRBs did not reach their maximum ductility limits of 25. The absolute maximum value of maximum ductility demand of BRBs of 3-story and 6-story BRBFs were about 32.1 and 32.3 under LA 18 and LA 16 ground motions, respectively. However, this may not be an indication of failure of BRBs because most prior isolated BRB tests [6] were carried out under smaller maximum ductility demand (10–25) and high cumulative ductility demand (approximately 300–1600), as opposed to the smaller cumulative ductility demand (43.6–144.1) but higher maximum ductility demand (29.4–35.6) observed in the time-history analyses under MCE ground motions.

6. Summary and conclusions

A direct design methodology, called performance-based plastic design (PBPD), based on energy–work balance, pre-selected target drift and yield mechanism was developed in this study to achieve predictable behavior of BRBFs by incorporating the inelastic characteristics of components in the design. The PBPD design procedure is not too different from what is done in current practice, yet it can be readily incorporated within the context of broader

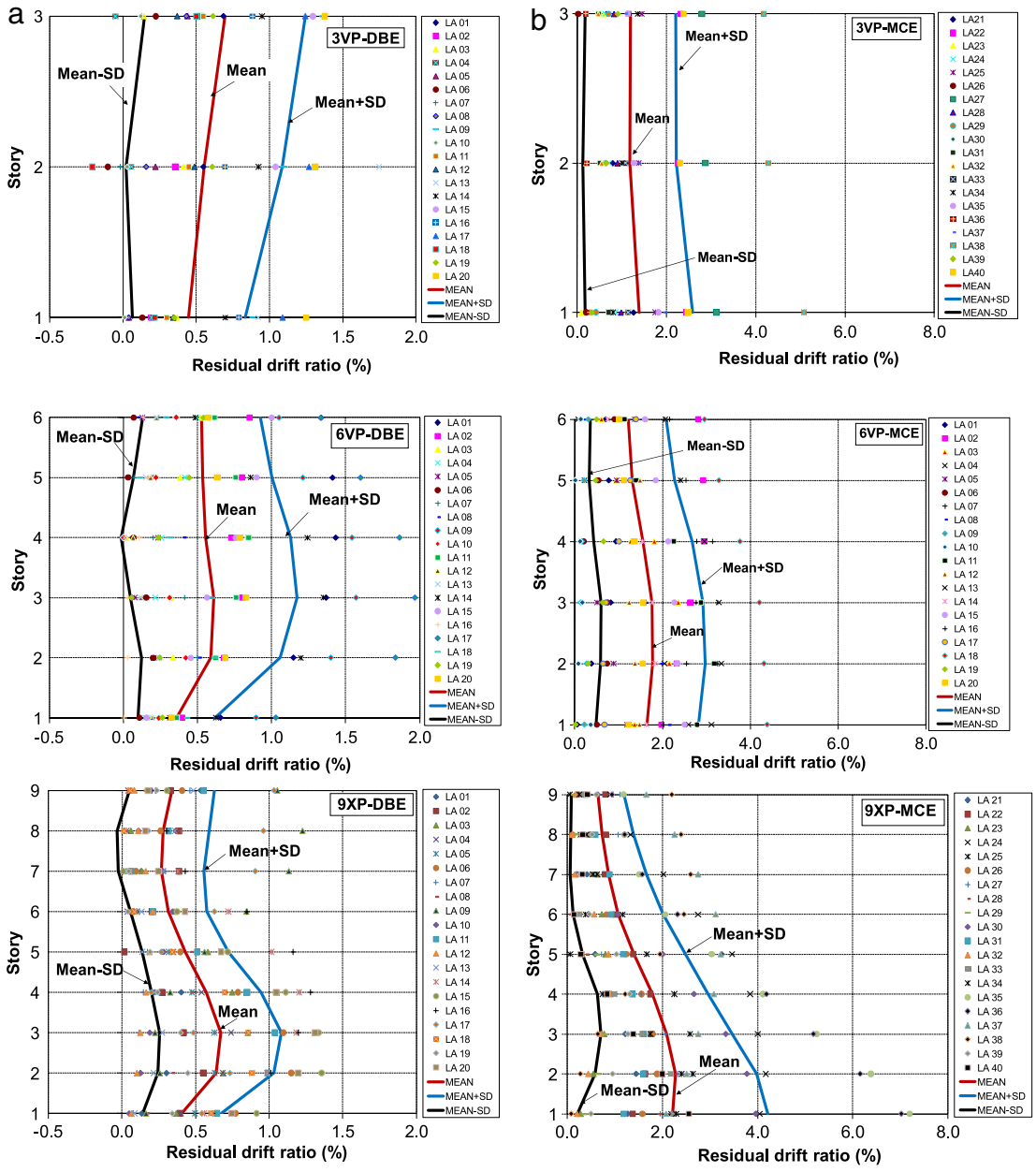

Fig. 9. Residual drift response of BRBFs (a) DBE (b) MCE.

Performance-Based Earthquake Engineering (PBEE) framework. It does differ from the way PBEE is practiced currently, which usually starts with an initial design according to conventional elastic design procedures using applicable design codes, followed by cumbersome and time-consuming iterative assessment process by using inelastic static or dynamic analyses till the desired performance objectives are achieved. The iterations are carried out in a purely trial-and-error manner. No guidance is provided to the designer as to how to achieve the desired goals such as, controlling drifts, distribution and extent of inelastic deformation, etc. In contrast, the PBPD method is a direct design method, which generally requires no evaluation after the initial design because the nonlinear behavior and key performance criteria are built into the design process from the beginning. In this study, this design methodology is applied to three low-to-medium rise BRBFs and the robustness and versatility of this method was evaluated by the seismic performance of these BRBFs under forty recorded ground motions representing the DBE and the MCE hazard levels. Following conclusions are drawn from the present study:

1. BRBFs designed as per PBPD methodology can successfully limit the maximum drifts within the pre-selected target drift level (1.75%), as well as achieve the intended yield mechanism under the DBE hazard level. The maximum drifts are generally uniformly distributed along the building height.
2. Mean values of maximum story drift ratios of the study BRBFs under the MCE hazard level are approximately 4%. However, previous experimental studies have shown that a well-detailed BRBF will experience minor damage at this drift level.
3. No iteration is required to achieve the desired performance objectives of all BRBFs since the inelastic characteristics of structural components and target drift ratio are directly considered in the design. Further, due to well-controlled drift, it is possible to achieve the desired seismic performance by neglecting additional force due to *P*-Delta effect in the design for simplicity.
4. The PBPD design base shears for the 3-, 6-, and 9-story BRBFs are 91%, 57%, and 64% of that calculated based on the modern codes.

This indicates that a more economical design can be realized by the PBPD method, while maintaining the desirable seismic performance.

References

[1] López WA, Sabelli R. Seismic design of buckling-restrained braced frames. Steel tips. Moraga (CA): Structural Steel Educational Council; 2004.

[2] Huang YC, Tsai KC. Experimental responses of large scale buckling restrained brace frames. Report no. CEER/R91-03. National Taiwan University; 2002 [in Chinese].

[3] Richard RM. Braced frame steel structures 402: when and why frame action matters. Struct Eng 2009.

[4] Uang CM, Nakashima M. Steel buckling-restrained braced frames. In: Earthquake engineering: recent advances and applications. Boca Raton (FL): CRC Press; 2000.

[5] Sabelli R. Research on improving the design and analysis of earthquake resistant steel braced frames. Final report—NEHRP Fellowship in Earthquake Hazard Reduction; 2000.

[6] Fahnestock LA, Ricles JM, Sause R. Experimental evaluation of a large-scale buckling-restrained braced frame. J Struct Eng 2007;133(9):1205–14.

[7] Prasad BK. Current status of buckling-restrained braced frame design: currently available buckling-restrained braces. In: Proceedings of 72nd annual convention. SEAOC. 2004.

[8] Federal Emergency Management Agency. FEMA. Next-generation performance-based seismic design guidelines—program plan for new and existing buildings. FEMA-445. Washington (DC); 2006.

[9] Housner G. Limit design of structures to resist earthquakes. In: Proceedings of the first world conference on earthquake engineering. 1956.

[10] Lee SS, Goel SC. Performance-based design of steel moment frames using target drift and yield mechanism. Report no. UMCEE 01-17; MI: University of Michigan at Ann Arbor; 2001.

[11] Chao SH, Goel SC. Performance-based design of eccentrically braced frames using target drift and yield mechanism. AISC Eng J 2006;173–200. 3rd Quarter.

[12] Chao SH, Goel SC. Performance-based plastic design of special truss moment frames. AISC Eng J 2008;127–50. 2nd Quarter.

[13] CSI. PERFORM 3D user's manual-version 4.0. Berkeley, (CA): Computers and Structures Inc.; 2007.

[14] Goel SC, Chao SH. Performance-based plastic design—earthquake resistant steel structures. International Code Council; 2008. p. 261.

[15] Newmark NM, Hall WJ. Earthquake spectra and design. El Cerrito (CA): Earthquake Engineering Research Institute; 1982.

[16] ASCE 7-05. Minimum design load for buildings and other structures. Reston (VA): American Society of Civil Engineers; 2005.

[17] Sahoo DR, Chao SH. Performance-based plastic design for buckling-restrained braced frames. In: Proceedings of 9th US national and 10th canadian conference on earthquake engineering. 2010 [in press].

[18] Chao SH, Goel SC, Lee SS. A seismic design lateral force distribution based on inelastic state of structures. Earthq Spectra 2007;23(5):547–69.

[19] Merritt S, Uang CM, Benzoni G. Subassemblage testing of star seismic buckling-restrained braces. TR-2003/04. La Jolla (CA): Univ. of California at San Diego; 2003.

[20] AISC. ANSI/AISC 341-05. Seismic provisions for structural steel buildings. Chicago (IL): American Institute of Steel Construction; 2005.

[21] Gupta A, Krawinkler H. Prediction of seismic demands for SMRFs with ductile connections and elements. Report no. SAC/BD-99/06. Sacramento (CA): SAC Joint Venture; 1999.

[22] SEAOC. Recommended lateral force requirements and commentary. 7th ed. Sacramento (CA): Seismology Committee of Structural Engineers Association of California; 1999.

[23] Building Seismic Safety Council. BSSC. National earthquake hazard reduction program (NEHRP) recommended provisions for seismic regulations for new buildings and other structures—part 2: commentary. FEMA 450-1. Washington (DC): Federal Emergency Management Agency; 2003.

[24] AISC. ANSI/AISC 360-05. Specifications for structural steel buildings. Chicago (IL): American Institute of Steel Construction; 2005.

[25] Richards PW. Seismic column demand in ductile braced frames. J Struct Eng 2009;135(1):33–41.

[26] Thornton W, Muir LS. Design of vertical bracing connections for high-seismic drift. Modern Steel Construction; March 2009.

[27] Tremblay R, Bolduc P, Neville R, DeVall R. Seismic testing and performance of buckling restrained bracing systems. Canad J Civ Eng 2006;33:183–98.

[28] Somerville PG, Smith M, Punyamurthula S, Sun J. Development of ground motion time histories for phase 2 of the FEMA/SAC steel project. Report no. SAC/BD-97/04. Sacramento (CA): SAC Joint Venture; 1997.